

Rate of helicity production by solar rotation

Mitchell A. Berger

Department of Mathematics, University College London

Alexander Ruzmaikin

Jet Propulsion Laboratory, California Institute of Technology

Abstract. In recent years, solar observers have discovered a striking pattern in the distribution of coronal magnetic structures: northern hemisphere structures tend to have negative magnetic helicity, while structures in the south tend to have positive magnetic helicity. This hemispheric dependence extends from photospheric observations to in situ measurements of magnetic clouds in the solar wind. Understanding the source of the hemispheric sign dependence, as well as its implications for solar and space physics has become known as the solar chirality problem. Rotation of open fields creates the Parker spiral which carries outward 10^{47} Mx^2 of magnetic helicity (in each hemisphere) during a solar cycle. In addition, rough estimates suggest that each hemisphere sheds on the order 10^{45} Mx^2 in coronal mass ejections each cycle. Both the α effect (arising from helical turbulence) and the Ω effect (arising from differential rotation) should contribute to the hemispheric chirality. We show that the Ω effect contribution can be captured in a surface integral, even though the helicity itself is stored deep in the convection zone. We then evaluate this surface integral using solar magnetogram data and differential rotation curves. Throughout the 22 year cycle studied (1976 -1998) the helicity production in the interior by differential rotation had the correct sign compared to observations of coronal structures – negative in the north and positive in the south. The net helicity flow into each hemisphere over this cycle was approximately $4 \times 10^{46} \text{ Mx}^2$. For comparison, we estimate the α effect contribution; this may well be as high or higher than the differential rotation contribution. The subsurface helicity can be transported to the corona with buoyant rising flux tubes. Evidently only a small fraction of the subsurface helicity escapes to the surface to supply coronal mass ejections.

1. Introduction

Observations of helical magnetic structure in the photosphere, corona, and solar wind have attracted considerable interest (for recent reviews, see *Brown et al.* [1999]). This paper addresses the balance of magnetic helicity in the Sun and in the heliosphere. At present this balance is poorly known, even though the helicity balance may have important consequences for solar activity.

Activity in the Sun and cool stars originates in the magnetic fields generated by motions inside the convection zone. Regular motions, such as the differential rotation, and correlated contributions from random motions, such as the kinetic helicity, generate a regular, mean magnetic field. This process is called the mean-field dynamo, although fluctuating magnetic fields always accompany the mean field [Moffatt 1978, Krause & Rädler 1981, Zeldovich *et al.* 1983]. The dynamo does more than simply provide the solar magnetic field with flux and energy. It also gives the solar field a rich topological structure. Magnetic helicity, the best known index of topological complexity, measures twisting and linking of fields [Moffatt 1978, Berger & Field 1984]. Magnetic helicity is believed to play an important role in many areas of solar activity, for example, in coronal mass ejections [Low 1994, Rust 1994, Rust 1997, Martin & McAllister 1997]. The helicity of magnetic fields below the surface can be carried into the corona by newly emerging flux loops. After emergence the loops can gain more helicity via rotational motions at the photosphere. If an active region field as a whole continues to build up helicity over time, the active region may lose stability, resulting in a mass ejection.

Several different measurements of coronal structures show a hemispheric dependence. Spiral patterns are often observed in the plasma surrounding sunspots; in the north these tend to be counterclockwise, while in the south they tend to be clockwise [Richardson 1941, Ding *et al.* 1987]. Vector magnetograms of photospheric fields show negative current helicity in the north and positive in the south [Seehafer 1990, Pevtsov *et al.* 1995]. Prominence structures also have a hemispheric dependence: northern prominences again tend to have negative helicity (these have been called ‘dextral prominences’) [Martin *et al.* 1992, Rust & Kumar 1994, Rust 1994].

Meanwhile, the solar wind carries helicity outward in many forms. On the largest scales, helicity flows outward in the shape of the Parker spiral [Bieber *et al.* 1987a]. This helicity arises predominantly from the mean rotation of the Sun twisting the open field lines. Again, northern magnetic fields tend to have negative magnetic helicity, while southern magnetic fields tend to have positive helicity. In addition to the helicity of the Parker spiral, magnetic fluctuations carry further helicity away from the Sun [Bieber *et al.* 1987b]. Coronal mass ejections (CMEs) can eject helicity which may be found in magnetic clouds [Rust 1994, Kumar & Rust 1996]. Estimates give a helicity flow due to CMEs of the order 10^{45} Mx^2 each 11 year cycle.

This paper investigates where the helicity originates. We will be primarily concerned with magnetic helicity buildup in the solar dynamo. However, we briefly discuss whether there are other possibilities. Many theorists [e.g., Parker, 1993] have placed the solar dynamo deep at the base of the convection zone, near $r = 0.7 R_S$. Toroidal fields generated in this region can become buoyant and rise to the surface to form active region fields. One might ask whether the fields acquire additional helicity as they rise through the convection zone.

Coriolis forces will distort a rising magnetic flux tube into a kinked shape [Rust 1997]. In addition, the coriolis forces twist the field lines within the tube. Both kinks and internal twist carry helicity [Berger & Field 1984, Moffatt & Ricca 1992]. By

helicity conservation no net helicity is produced; the kink helicity and twist helicity must be equal in magnitude and opposite in sign. Coriolis forces in the north create positive kink helicity. Thus one might hope that the negative twist helicity might be observed in coronal loops. Unfortunately for this idea, when the tube emerges into the low beta corona, it takes a form consistent with its total helicity, rather than the separate contributions of twist and kink. If the total helicity were zero, for example, the tube would simply unkink and untwist as it emerges. In other words, because magnetic forces dominate in the corona, a coronal loop forgets the shape it once had below the surface where fluid forces dominate.

Various attempts have been made to see how large-scale surface motions (such as differential rotation) affect preexisting coronal fields [*van Ballegooijen & Martens* 1990, *Priest et al.* 1996]. Unfortunately, this process generates helicity of the wrong sign more often than the correct sign [*van Ballegooijen et al.* 1998]. For example, if the polarity inversion line of a polar crown prominence is oriented north-south, differential rotation yields the correct sign, but an east-west orientation yields the wrong sign. The negative results of these studies suggest most of the hemispheric asymmetry must originate below the photosphere. In this context, models are being developed for the formation of prominences from rising subsurface fields already carrying helicity [*Low* 1994, *Low & Hundhausen* 1995, *Priest et al.* 1996].

Of course, on smaller scales the generation of helicity in preexisting coronal fields can be important for determining the structure of individual coronal loops. The random rotation of photospheric foot points of loops will inject a root-mean-square twist helicity into the loops; this is accompanied by an increase in magnetic energy storage. Microflares resulting from reconnection between loops can tap this energy storage and contribute to coronal heating [*Sturrock & Uchida* 1981, *Parker* 1983, *Berger* 1991, *Karpen et al.* 1993].

Recently, the effect of kinetic helicity (the α effect) on magnetic helicity in the Sun has been considered [*Ruzmaikin* 1996, *Seehafer* 1996]. Kinetic helicity does not create a net magnetic helicity; instead, it creates helicities of opposite signs in the mean field and in the fluctuating field [see, e.g., *Moffatt*, 1978; *Zeldovich et al.*, 1983]. The sign of the kinetic helicity (and hence of the magnetic helicities generated) is a matter of some controversy and may vary from place to place [*Brandenburg et al.* 1990, *Brummell et al.* 1997]. If, as some simple theoretical arguments predict, the kinetic helicity is positive in the northern solar hemisphere and negative in the southern hemisphere, the mechanism produces mean field magnetic helicity positive in the north and negative in the south. To match observations, however, we need negative kinetic helicity in the north.

Another candidate for the source of helicity lies in the effect of differential rotation on deep subsurface fields [*Babcock* 1961, *Rust* 1997]. The main purpose of this paper is to measure this effect. We will show that the generation of magnetic helicity by differential rotation can be calculated directly from observations, with a minimum of theoretical simplifications. For example, differential rotation acts equally on any magnetic field, so

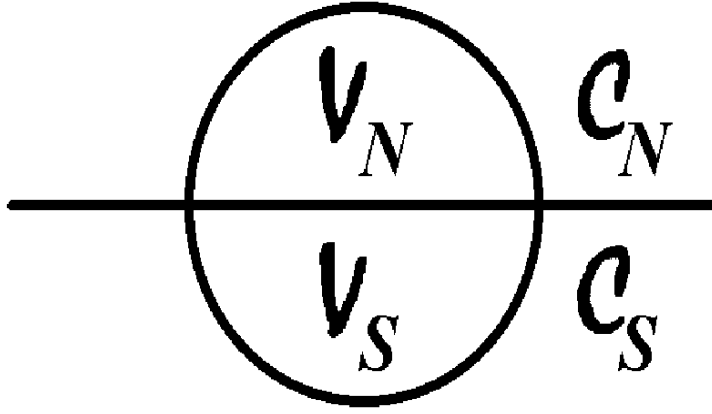


Figure 1. Divide space into four regions: the north solar interior \mathcal{V}_N with helicity $H_{\mathcal{V}_N}$, the south solar interior \mathcal{V}_S with helicity $H_{\mathcal{V}_S}$, the north corona \mathcal{C}_N with helicity $H_{\mathcal{C}_N}$, and the south corona \mathcal{C}_S with helicity $H_{\mathcal{C}_S}$.

there is no theoretical need to divide the field into mean and fluctuating components. We evaluate the observed rate of helicity transfer through the photosphere between the entire Sun and the heliosphere for an entire 22 year solar cycle (1976 to 1998). We also estimate the helicity buildup in the solar interior separately for the northern hemisphere and the southern hemisphere.

The paper proceeds as follows: Section 2 provides a theoretical introduction to magnetic helicity transfer through boundaries. As a further illustration, section 3 employs the helicity transfer equation to describe a rotating sphere with a dipole field. This provides a simple model for the Parker spiral, and complements the analysis of *Bieber et al.* [1987a]. While the main purpose of this paper is to directly calculate helicity flows through the photosphere and equator from observations, we do not wish to neglect the influence of the α effect. Section 4 gives a brief discussion of how the α effect may change the solar helicity balance. The analysis of solar data is described in section 5. This section contains the principal results of this paper. Conclusions will be presented in section 6.

2. Helicity Transfer Through Boundaries

We must introduce some notation to denote all the regions of space we will be dealing with (see figure 1). First, \mathcal{V} refers to the entire interior volume of the Sun below the photosphere. The northern hemisphere of this interior volume is \mathcal{V}_N , while the southern hemisphere is \mathcal{V}_S . The net magnetic helicities contained within these regions will be called $H_{\mathcal{V}}$, $H_{\mathcal{V}_N}$, and $H_{\mathcal{V}_S}$. Space outside the photosphere (e.g., chromosphere, corona, heliosphere, and beyond) will simply be called the corona, with the symbol \mathcal{C} . The northern half of this exterior volume is \mathcal{C}_N , and the southern half is \mathcal{C}_S . Suppose magnetic helicity is transferred through the photosphere (as discussed in subsequent sections). The rate at which helicity transfers from \mathcal{V} to \mathcal{C} will be called $\dot{H}(\mathcal{V} \rightarrow \mathcal{C})$, so

that

$$\frac{dH_{\mathcal{C}}}{dt} = \dot{H}(\mathcal{V} \rightarrow \mathcal{C}); \quad (1)$$

$$\frac{dH_{\mathcal{V}}}{dt} = \dot{H}(\mathcal{C} \rightarrow \mathcal{V}). \quad (2)$$

By helicity conservation, $\dot{H}(\mathcal{C} \rightarrow \mathcal{V}) = -\dot{H}(\mathcal{V} \rightarrow \mathcal{C})$. The purpose of this paper is to calculate the various helicity transfers between the four regions due to differential rotation, using observations of magnetic flux distributions at the photosphere.

The magnetic helicity measures the net linking of field lines with each other [Moffatt 1978]. First, consider the helicity H integrated over all space. In this case, no field lines have endpoints on boundaries; in effect, all field lines eventually close upon themselves to form closed curves (ergodic field lines form very close approximations to closed curves [Arnold & Khesin 1998]). If two bundles of closed field lines link each other, their linking (multiplied by the product of the fluxes) will add to the helicity.

Suppose, however, we consider the field lines in a subregion of space (e.g., the solar interior). In general, these lines will have endpoints on the boundaries of the subregion (e.g., the photosphere). The definition of helicity requires some care because of this. The photospheric boundary is not a magnetic surface (on a magnetic surface the normal field component $B_n = 0$). We note that the flux B_n at the boundary of any volume \mathcal{V} uniquely defines a potential field \mathbf{P} within \mathcal{V} . Potential fields have no currents (except for surface currents in the boundaries) and are the absolute minimum energy state of all fields with the same boundary flux. Thus comparing the actual field inside \mathcal{V} with the corresponding potential field tells us about both the distribution of currents in \mathcal{V} and the magnetic energy stored within \mathcal{V} . The potential field inside a volume \mathcal{V} can be regarded as the ground state (it is sometimes called the vacuum field), given the boundary function B_n .

The magnetic helicity in any volume \mathcal{V} becomes a unique and well-defined topological measure when we set the helicity of the corresponding potential field to zero [Berger & Field 1984, Finn & Antonsen 1985]. The formula for the helicity is

$$H_{\mathcal{V}} = \int_{\mathcal{V}} (\mathbf{A} + \mathbf{A}_P) \cdot (\mathbf{B} - \mathbf{P}) d^3x. \quad (3)$$

One may check that $H_{\mathcal{V}}$ vanishes for potential fields $\mathbf{B} = \mathbf{P}$ and that $H_{\mathcal{V}}$ is invariant to gauge transformations $\mathbf{A} \rightarrow \mathbf{A} + \nabla\phi$. The quantity $H_{\mathcal{V}}$ measures the amount of twisting and linking of field lines within the volume \mathcal{V} .

The time derivative of the helicity in the Sun (or any other volume \mathcal{V}) satisfies an equation reminiscent of Poynting's theorem:

$$\frac{dH_{\mathcal{V}}}{dt} = -2 \int_{\mathcal{V}} \mathbf{E} \cdot \mathbf{B} d^3x + 2 \oint_{\text{boundary}} \mathbf{A}_P \times \mathbf{E} \cdot \hat{n} d^2x, \quad (4)$$

where \mathbf{E} is the electric field. We consider a plasma with a simple Ohm's law:

$$\mathbf{E} = \mathbf{B} \times \mathbf{v} + \eta \mathbf{J}. \quad (5)$$

The first integral in (4) describes the dissipation of helicity due to the dissipation coefficient η . Strict limits can be placed on magnetic helicity dissipation [Berger 1984];

for magnetic systems undergoing reconnection the dissipation is negligible. Helicity dissipation in the context of the α dynamo will be discussed further in section 4. For now, however, we will concentrate on the boundary integral.

As the evaluation of the second integral in (4) is the topic of this paper, we review its properties in detail. This integral describes the transfer of helicity across the boundary and involves the boundary flux B_n and the plasma velocity \mathbf{v} [Berger & Field 1984]:

$$\frac{dH_V}{dt} = 2 \oint (\mathbf{A}_P \cdot \mathbf{v}) B_n d^2x - 2 \oint (\mathbf{A}_P \cdot \mathbf{B}) v_n d^2x. \quad (6)$$

The normal component of the velocity contributes only to the second integral in (6). This integral corresponds to the bulk transport of plasma carrying helical fields across the surface. For example, a newly emerging twisted loop transports helicity from the convection zone to the corona. In the interior of the Sun, transport of flux from the northern hemisphere to the southern hemisphere can also contribute to the second integral. In this paper, however, we will concentrate on differential rotation, which involves only the first integral.

The vector field \mathbf{A}_P depends totally on B_n and the shape of the boundary. In particular, \mathbf{A}_P satisfies the three conditions

$$\nabla \times \mathbf{A}_P = \mathbf{P}, \quad (7)$$

$$\nabla \cdot \mathbf{A}_P = 0, \quad (8)$$

$$\mathbf{A}_P \cdot \hat{\mathbf{n}} = 0. \quad (9)$$

If the boundary is a plane or a sphere, then condition (8) becomes $\nabla_{\parallel} \cdot \mathbf{A}_P = 0$, where ∇_{\parallel} is the gradient parallel to the surface. In this case [Bogomolov 1979, Kimura & Okamoto 1987] these conditions have a unique solution $\mathbf{A}_P = \hat{\mathbf{n}} \times \nabla \psi$, where $\Delta \psi = -B_n$, with Δ being the surface Laplace operator. For planar boundaries,

$$\psi(\mathbf{x}) = -\frac{1}{2\pi} \int B_n(\mathbf{x}') \ln |\mathbf{x} - \mathbf{x}'| d^2x', \quad (10)$$

and for spherical boundaries of radius R ,

$$\psi(\theta, \phi) = -\frac{R^2}{4\pi} \oint B_n(\theta', \phi') \ln \frac{1 - \cos \xi}{2} d^2x', \quad (11)$$

where ξ is the spherical distance between (θ, ϕ) and (θ', ϕ') :

$$\cos \xi = \cos \theta \cos \theta' + \sin \theta \sin \theta' \cos(\phi - \phi'). \quad (12)$$

For spherical boundaries it is often convenient to employ spherical harmonics. Thus we expand the surface field as

$$B_r = \sum_{\ell m} b_{\ell m} Y_{\ell}^m. \quad (13)$$

The corresponding vector potential is

$$\mathbf{A}_P = \sum_{\ell m} \frac{-R b_{\ell m}}{\ell(\ell+1)} \mathbf{r} \times \nabla Y_{\ell}^m. \quad (14)$$

To calculate the helicity transfers, we calculate integrals of $(\mathbf{A}_P \cdot \mathbf{v}) B_n^*$. With \mathbf{A}_P and B_n presented as a sum of spherical harmonics, the integrals involve combinations

of different values of mode numbers ℓ and m . Suppose $\mathbf{A}_P \sim e^{im\phi}$ and $B_n \sim e^{in\phi}$. Then integration over azimuthal angle ϕ eliminates all combinations with $n \neq m$ (as \mathbf{v} is independent of ϕ). Thus we can calculate \dot{H} for each azimuthal m mode separately. However, because \mathbf{v} does depend on θ , the poloidal wave numbers ℓ do not separate.

Axial symmetry (where the magnetic field is independent of the coordinate ϕ) considerably simplifies the calculations. For planar boundaries with $\Phi(r)$ denoting the net flux within radius r and $\hat{\phi}$ denoting the angular direction,

$$\mathbf{A}_P(r) = \frac{\Phi(r)}{2\pi r} \hat{\phi}, \quad \Phi(r) = 2\pi \int_0^r B_z r' dr'. \quad (15)$$

For spherical boundaries with net flux $\Phi(\theta)$ between the north pole and colatitude θ ,

$$\mathbf{A}_P(\theta) = \frac{\Phi(\theta)}{2\pi R \sin \theta} \hat{\phi}, \quad \Phi(\theta) = 2\pi \int_0^\theta B_r \sin \theta' d\theta'. \quad (16)$$

Consider, for example, helicity transfer into the northern hemisphere due to a velocity $\mathbf{v} = \Omega(r, \theta)r \sin \theta \hat{\phi}$. Equations (6), (15), and (16) give

$$\begin{aligned} \frac{dH_{\mathcal{V}N}}{dt} &= 2R^2 \int_0^{\pi/2} B_r(\theta) \Phi(\theta) \Omega(R, \theta) \sin \theta d\theta \\ &+ 2 \int_0^{R_S} B_\theta(r) \Phi(r) \Omega(r, \pi/2) r dr. \end{aligned} \quad (17)$$

The first term describes the contribution from differential rotation at the surface, while the second term describes rotation at the equator.

3. Example: A Rotating Sphere With A Dipole Field

To illustrate the helicity transfer equations (4) and (6), we consider a uniformly rotating sphere with a dipole field. If the sphere is surrounded by a vacuum, then the magnetic field is static and there is no electric field. Consequently, $\mathbf{A}_P \times \mathbf{E} = 0$, and there is no transfer of helicity across the surface. On the other hand, if the sphere is surrounded by a plasma, then $\mathbf{E} = \mathbf{B} \times \mathbf{v}$. Consider a simple model of the Sun, radius R_S , rotating with uniform angular velocity Ω_0 and exhibiting a photospheric dipole field $B_n = B_1 \cos \theta$. Then $\mathbf{v} = R_S \Omega_0 \sin \theta \hat{\phi}$, and

$$\frac{dH_{\mathcal{V}}}{dt} = 2 \oint_{\text{photo}} (\mathbf{A}_P \cdot \mathbf{v}) B_n d^2x \quad (18)$$

$$\frac{dH_{\mathcal{V}}}{dt} = 2R_S \Omega_0 \oint_{\text{photo}} B_1 A_{P\phi} \sin \theta \cos \theta d^2x. \quad (19)$$

To obtain \mathbf{A}_P , we use (14) or (16) with $b_{10} = \sqrt{4\pi/3} B_1$. This gives $A_{P\phi} = (B_1 R_S / 2) \sin \theta$. By conservation of helicity, $dH_C/dt = -dH_{\mathcal{V}}/dt$.

The integral may now be evaluated; the result is simply $dH_{\mathcal{V}}/dt = dH_C/dt = 0$. Evidently, our simple model is too symmetric to yield any net helicity transfer. We evidently need to look at the northern and southern hemispheres separately. *Bieber et al.* [1987a] have demonstrated that negative helicity propagates out into the north solar

wind and positive helicity propagates into the south wind. Let us divide space up into four regions (Figure 1), as explained at the end of section 1.

Motions at the boundaries between the four subregions of space transfer helicity according to

$$dH_{\mathcal{C}_S}/dt = \dot{H}(\mathcal{V}_S \rightarrow \mathcal{C}_S); \quad (20)$$

$$dH_{\mathcal{V}_S}/dt = \dot{H}(\mathcal{V}_N \rightarrow \mathcal{V}_S) - \dot{H}(\mathcal{V}_S \rightarrow \mathcal{C}_S); \quad (21)$$

$$dH_{\mathcal{V}_N}/dt = \dot{H}(\mathcal{C}_N \rightarrow \mathcal{V}_N) - \dot{H}(\mathcal{V}_N \rightarrow \mathcal{V}_S); \quad (22)$$

$$dH_{\mathcal{C}_N}/dt = -\dot{H}(\mathcal{C}_N \rightarrow \mathcal{V}_N). \quad (23)$$

Let us discuss this helicity transfer in detail. The sign of helicity transfer can be schematically described by letting a double arrow denote the direction of transfer of positive helicity. We will show that this direction is

$$\mathcal{C}_N \Rightarrow \mathcal{V}_N \Rightarrow \mathcal{V}_S \Rightarrow \mathcal{C}_S \quad (24)$$

(we will not consider any transfers of helicity directly between \mathcal{C}_N and \mathcal{C}_S at their mutual boundary, as these involve the velocity field in the solar wind, rather than the rotation of the Sun).

First, consider the helicity transfer $\mathcal{C}_N \Rightarrow \mathcal{V}_N$. This is caused by the rotation of the photospheric boundary between \mathcal{C}_N and \mathcal{V}_N . By conservation of helicity, no net helicity is produced. Instead, negative helicity in the form of a helical wave flows outward into the solar wind. At the same time, positive helicity flows inward into the north interior \mathcal{V}_N . We can calculate the magnitude of these equal and opposite helicity flows as in (19).

In order to get the signs right, we need to know the direction of \hat{n} in the helicity transfer equations. The normal \hat{n} points out of the volume whose helicity time derivative is being calculated. Thus, if we are calculating $dH_{\mathcal{V}}/dt$, then \hat{n} points out of the Sun, that is, in the positive radial r direction. On the other hand, if we wish to calculate $dH_{\mathcal{C}}/dt$, then $\hat{n} = -\hat{r}$.

Applying the helicity transfer equations to the north photospheric boundary between \mathcal{V}_N and \mathcal{C}_N , with $\mathbf{v} = R_S \Omega_0 \sin \theta \hat{\phi}$, we find

$$\frac{dH_{\mathcal{C}_N}}{dt} = \dot{H}(\mathcal{V}_N \rightarrow \mathcal{C}_N) = -\dot{H}(\mathcal{C}_N \rightarrow \mathcal{V}_N) \quad (25)$$

$$\frac{dH_{\mathcal{C}_N}}{dt} = -2 \int_{\text{north photo}} (\mathbf{A}_P \cdot \mathbf{v}) B_r d^2x \quad (26)$$

$$\frac{dH_{\mathcal{C}_N}}{dt} = -\frac{\Omega_0}{2\pi} \Phi^2 \quad (27)$$

where $\Phi = \pi R_{\odot}^2 B_1$ is the net dipole flux through the north photosphere. In general, H/Φ^2 measures the net twist (number of turns through 2π radians) of a twisted flux tube. Thus the northern solar wind receives one negative twist per solar rotation from the photosphere. To balance this, the north solar interior receives one positive twist from the photosphere. This explains why the double arrow (direction of positive helicity flow) in (24) points from \mathcal{C}_N to \mathcal{V}_N . This result agrees exactly with estimates of the net magnetic helicity contained in the Parker spiral [Bieber *et al.* 1987a].

However, the net helicity change in the north solar interior is zero, as there is an additional boundary contributing to the change. The boundary between \mathcal{V}_N and \mathcal{V}_S is the equatorial plane inside the Sun. This plane rotates (in the present simple example) with uniform angular velocity Ω_0 . As a consequence, field lines passing through the equator receive a twist once each solar rotation: a negative twist above in \mathcal{V}_N and a positive twist below in \mathcal{V}_S . The net flux passing through the equator is still Φ . Thus (as can be verified from (6) and (15)) $\dot{H}(\mathcal{V}_S \rightarrow \mathcal{V}_N) = -(\Omega_0/2\pi)\Phi^2$. This cancels out the photospheric contribution $\dot{H}(\mathcal{C}_N \rightarrow \mathcal{V}_N)$ and shows that the double arrow in (24) points from \mathcal{V}_N to \mathcal{V}_S . Finally, the southern heliosphere \mathcal{C}_S is at the end of the line; it steadily gains positive helicity. Similar calculations show that the southern solar wind receives one positive twist per rotation.

To summarize, for uniform rotation all the transfers are equal in magnitude. There is no net buildup of helicity in either \mathcal{V}_N or \mathcal{V}_S . However, the south solar wind gains helicity, which propagates out to infinity in the solar wind. Similarly, the north solar wind loses helicity, or, more properly, negative helicity propagates out to infinity. The helicity flowing out of the northern photosphere can be interpreted geometrically [Bieber *et al.* 1987a]. Because of the solar rotation, the large-scale field of the solar wind appears as the Parker spiral: at low latitudes, field lines have the shape of outward propagating spirals, while at high latitudes the field lines have helical shapes.

4. The α Effect

Here we briefly review how the α term in the solar dynamo affects helicity distribution. In solar dynamo theory, turbulent flows regenerate poloidal magnetic flux from the toroidal field [Moffatt 1978, Krause & Rädler 1981, Zeldovich *et al.* 1983]. The effect of the turbulence is highly nonlinear; but to a first approximation the flows create an effective electromotive force

$$\xi = \alpha \mathbf{B} - \beta \nabla \times \mathbf{B}. \quad (28)$$

Here \mathbf{B} is the mean magnetic field. In classical dynamo theory, α arises from kinetic helicity while β represents a turbulent diffusion. The electric field appearing in (4) becomes $\mathbf{E} = -\xi$. Thus [Seehafer 1996, Ruzmaikin 1996] the α effect can change the helicity of the mean field. From (4) we have

$$\begin{aligned} \frac{dH_V}{dt} &= 2 \int_V (\alpha B^2 - \beta \nabla \times \mathbf{B} \cdot \mathbf{B}) d^3x \\ &\quad - 2 \oint \mathbf{A}_P \times (\alpha \mathbf{B} - \beta \nabla \times \mathbf{B}) \cdot \hat{n} d^2x. \end{aligned} \quad (29)$$

The first (volume) term represents nonlinear transfer of helicity between the mean field and the fluctuating field; no net helicity is created. Both the sign and the value of α are subjects of intense debate [Brandenburg *et al.* 1990, Brummell *et al.* 1997]. As the rotation rate decreases with depth in the overshoot layer, there are indications that α should be negative there (in the north); otherwise, the butterfly diagrams would be reversed [Moffatt 1978]. This would imply that the α term gives the same sign of helicity

generation as differential rotation (giving the correct sign as observed in the corona and solar wind).

The magnitude of this term can be quite high. Consider a dynamo operating in the convective overshoot layer of the Sun between the equator and, say, $\theta = \pi/4$. If this layer has a thickness of 10^4 km, then $2 \int_V (\alpha B^2) d^3x \approx 2 \times 10^{36} \alpha B^2 \text{ Mx}^2/\text{d}$. Fairly small values for α and B are needed to match generation by differential rotation: e.g. $\alpha = 0.1$ cm/s and $B = 10^4$ G give $10^{43} \text{ Mx}^2/\text{d}$. This is comparable to the differential rotation results discussed below and an order of magnitude higher than the estimated helicity loss in CMEs [Rust 1997]. On the other hand, α effect generation may be inhibited by several factors, for example, the β term, variations in the sign of α from place to place, and inhibition of fluid turbulence by the magnetic field.

What is the fate of the magnetic helicity transferred to the fluctuating magnetic field? In Kolmogorov turbulence theory, energy cascades to small scales, where it can be dissipated by viscosity. Similarly, in MHD turbulence, magnetic energy can cascade to small scales owing to turbulent processes. However, magnetic helicity does not easily fit into small scales. In fact, theory and numerical simulations [Pouquet *et al.* 1976, Matthaeus & Montgomery 1980] suggest that magnetic helicity cascades in the wrong direction to larger length scales, that is, inverse cascades. Thus, while the α and β terms represent transfer of helicity between large (e.g., $10^4 - 10^5$ km for the Sun) and intermediate scales (e.g., $10^2 - 10^3$ km), further transfer to dissipation length scales may be inhibited. At the base of the convection zone the plasma is hot ($T = 2 \times 10^6$ K), and, consequently, the Spitzer resistive diffusion coefficient is small, $\eta = 3 \times 10^3 \text{ cm}^2/\text{s}$. Magnetic helicity stored in structures with a length scale λ will dissipate in a time $\tau_d = \lambda^2/\eta$. If we let $\tau_d = 11$ years, then $\lambda = 10$ km. If magnetic helicity cannot cascade down to this length scale, then dissipation of fluctuating magnetic helicity will be relatively inefficient. Of course, in this paper we mostly discuss rates of change of the magnetic helicity content of solar fields, rather than the actual amount of helicity stored at any one time. If the helicity storage is high, then dissipation can be comparable in magnitude to generation even if the magnetic helicity stays at length scales larger than $\lambda = 10$ km.

The second term in (29) represents turbulent diffusion of magnetic helicity across boundaries. If we apply the equation to the northern interior of the Sun, the boundaries are the photosphere and the equator. Presumably buoyancy is more important than turbulent diffusion in bringing helical fields through the photosphere. Also, we know the magnitude of helicity flow upwards carried by emerging flux; it can be estimated from the CME rate. However, diffusion of helicity across the equator due to turbulent motions may be quite important for the global helicity balance. Here negative helicity from the north cancels with positive helicity from the south. The diffusion across the equator is

$$\dot{H}(\mathcal{V}_N \rightarrow \mathcal{V}_S) = 2 \int_{eq} \mathbf{A}_P \times (\alpha \mathbf{B} - \beta \nabla \times \mathbf{B}) \cdot \hat{\theta} d^2x. \quad (30)$$

Let us give a crude estimate of this term. For a symmetric mean field \mathbf{A}_P will have only a ϕ component (see (15)), while the radial component of \mathbf{B} vanishes at the equator. Thus the α term does not contribute. Meanwhile, the radial component of $\nabla \times \mathbf{B}$ is $(1/r)\partial B_\phi/\partial\theta \approx B/R_S$. Again, we consider a thin (10^4 km) layer dynamo at the base of the convection zone, $r = 5 \times 10^5$ km. With $B = 10^4$ G and $2\pi r \mathbf{A}_P \approx 2 \times 10^{22}$ Mx, one obtains $\dot{H}(\mathcal{V}_N \rightarrow \mathcal{V}_S) = 10^{30} \beta \text{Mx}^2/\text{day}$. Thus a turbulent diffusivity of $\beta \approx 10^{13} \text{cm}^2/\text{s}$ will make the equatorial diffusion term comparable in magnitude to the volume α effect term and the helicity flow due to differential rotation.

5. Analysis Of Solar Data

5.1. Data Sets

The latitudinal distribution of the solar surface rotation is known from direct optical observations, while the radial distribution is determined from helioseismic analyses of frequency splitting of acoustic oscillations (for the latest results and references, see *Kosovichev et al.* [1997, Figure 13] and *Charbonneau et al.*, (preprint, 1999)). The radial gradient of angular velocity at the solar equator is very small through almost the whole convection zone and is positive near the bottom of the convection zone. We will adopt the Charbonneau analytical fit

$$\begin{aligned}\Omega(r, \theta) &= \Omega_c + \frac{1}{2} \left[1 + \text{erf} \left(2 \frac{r - r_c}{d_1} \right) \right] (\Omega_s(\theta) - \Omega_c); \\ \Omega_s(\theta) &= \Omega_{eq} + a_2 \cos^2 \theta + a_4 \cos^4 \theta,\end{aligned}\tag{31}$$

where $\Omega_{eq}/2\pi = 460.7$ nHz, $\Omega_c/2\pi = 432.8$ nHz, $a_2/2\pi = -62.69$ nHz, $a_4/2\pi = -67.13$ nHz, $r_c = 0.7 R_S$, and $d_1 = 0.05 R_S$. The function $\Omega_s(\theta) = \Omega(R_S, \theta)$ gives the surface distribution. The surface and equator velocity fields corresponding to Ω are

$$\mathbf{v} = \begin{cases} \Omega(R, \theta) R \sin \theta \hat{\phi}, & \text{Surface} \\ \Omega(r, \pi/2) r \hat{\phi} & \text{Equator.} \end{cases}\tag{32}$$

We employ the observations of photospheric magnetic fields obtained by the Wilcox observatory, from Carrington rotation CR1643 to CR1949. The radial field in the Wilcox data has been inferred from the line-of-sight field assuming a potential field between the photosphere and a radial field source surface at $3.25R$. This method has been successful in predicting the large-scale interplanetary magnetic field structure at 1 AU [Hoeksema et al 1983; Zhao & Hoeksema 1993, 1995; Wang, 1993]. The potential field approximation may, of course, be a source of systematic error. This should be most pronounced for fields in active regions, where there is the most current buildup. This presumably affects the high harmonic modes the most; fortunately these contribute only a few percent of the total helicity flow. Another difficulty lies in compensating for saturation of the Fe I spectral lines. *Zhao & Hoeksema* [1993, 1995] suggest that a saturation correction factor of 1.8 is most consistent with solar wind observations; we employ this factor in our analysis.

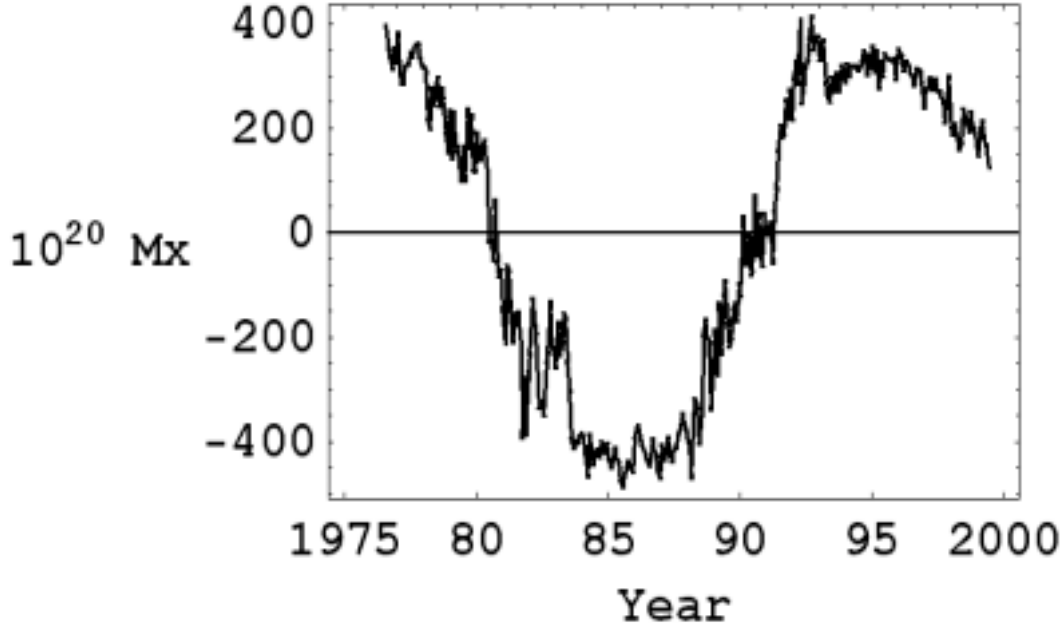


Figure 2. Net magnetic flux through the northern hemisphere. The units are 10^{20} Mx.

The Wilcox observatory provides spherical harmonic coefficients up to mode numbers $\ell = 9$, $m = 9$. This harmonic analysis conveniently allows us to employ (13) and (14) for the fields. In practice, the cutoff at 9 modes probably changes our results by only a few percent: we find that the high modes add negligible contributions to the total helicity flows.

As we do not know the B_θ distribution in the interior of the Sun at the equator, we simply assume that the net flux (obtained from the photospheric data) is uniformly distributed at the base of the convection zone, between $r = 0.68R$ and $r = 0.7R$. The net differential rotation at the equator is small; as a result, our assumption gives an effective rotation rate of $\Omega = 0.98\Omega_{eq}$. (In other words, the helicity transfer across the equator is equal to that obtained if the equator rotated rigidly with $\Omega = 0.98\Omega_{eq}$.) If magnetic flux were uniformly distributed as a function of depth, the helicity transfer would increase only by 1% (this would be in the direction of increasing the magnitude of the helicity transfers into the northern and southern hemispheres).

5.2. Formation of the Parker Spiral

The Sun has a net open flux Φ emanating from the northern hemisphere into interplanetary space (with an equal and opposite flux emanating from the southern hemisphere). Figure 2 shows the net northern flux Φ as a function of time. The overall solar rotation imparts one complete twist to this flux each rotation period

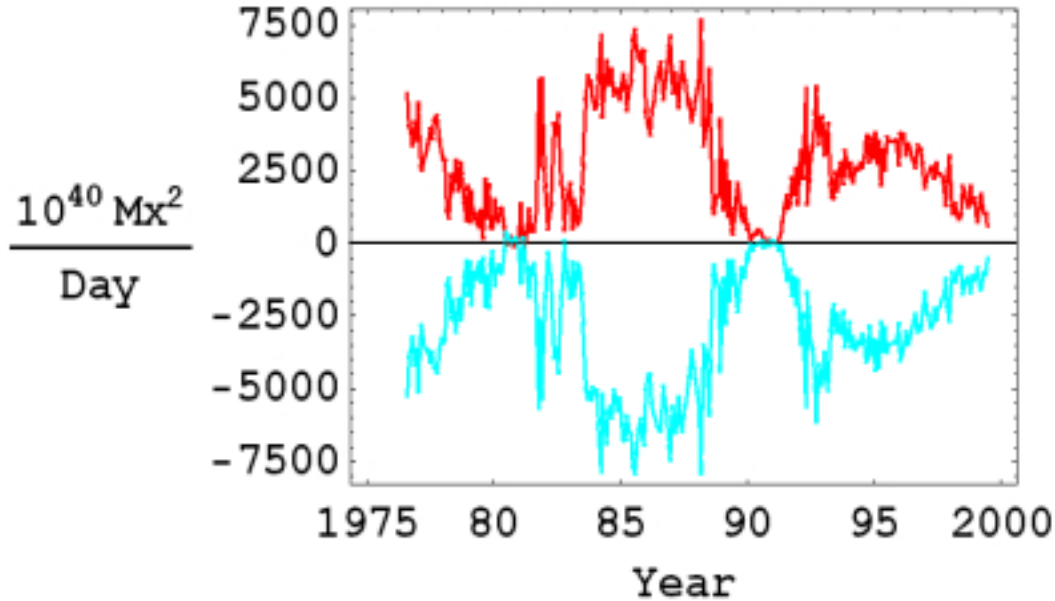


Figure 3. Net transfer of helicity into the southern corona and wind $dH_{CS}/dt = \dot{H}(\mathcal{V}_S \rightarrow \mathcal{C}_S)$ (predominantly positive curve), and into the northern corona and wind $dH_{CN}/dt = \dot{H}(\mathcal{V}_N \rightarrow \mathcal{C}_N)$ (predominantly negative curve). The units are $10^{40} \text{ Mx}^2/\text{day}$.

[Bieber *et al.* 1987a]. Figure 3 shows the helicity flows into the north and south solar wind over the past 22 years. Figure 3 provides a clear confirmation of the results of Bieber *et al.*, using quite different methods. In particular, we are observing the source of the helicity flow at the photosphere, while Bieber *et al.* considered in situ observations of the solar wind.

The helicity flows in Figure 3 closely correlate with the solar cycle. The sign does not depend on which 11 year sunspot cycle the data comes from. (This independence of cycle can be most clearly seen in the simple dipole model of section 3; the helicity transfer involves the square of the net flux rather than the sign of the flux). They are maximum in magnitude at solar minimum, when the poloidal field is strongest (e.g., in 1985, Φ reached its maximum magnitude $-4.85 \times 10^{22} \text{ Mx}$).

The data show fluctuations on smaller timescales than the solar cycle for both flux and helicity flow; at the present time we do not know the cause of these fluctuations. We note that over the time period of our data set the helicity flow into the south corona and wind has been stronger in magnitude than the north. It is possible that this discrepancy can also be measured using solar wind observations. The asymmetry between north and south may also have some significance for dynamo modeling.

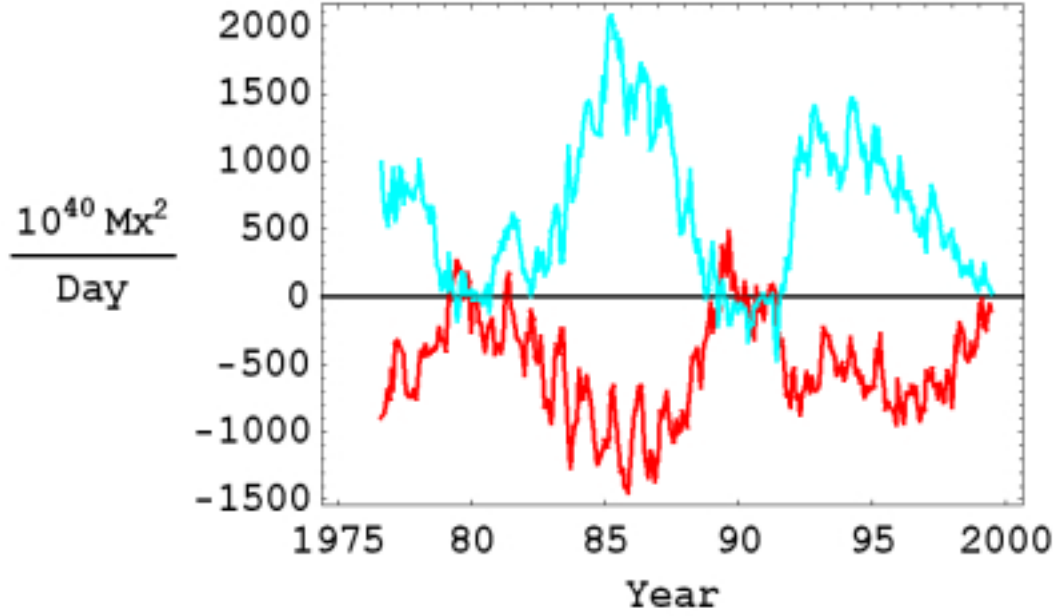


Figure 4. Helicity transfer into the southern interior (predominantly positive curve) $dH_{VN}/dt = \dot{H}(C_N \rightarrow \mathcal{V}_N) - \dot{H}(\mathcal{V}_N \rightarrow \mathcal{V}_S)$ and northern interior (predominantly negative curve) $dH_{VS}/dt = \dot{H}(\mathcal{V}_N \rightarrow \mathcal{V}_S) - \dot{H}(\mathcal{V}_S \rightarrow C_S)$. The differences in magnitude between the two curves go up to $5 \times 10^{42} \text{ Mx}^2/d$.

5.3. Transfer of Helicity Into the Northern and Southern Solar Interior

Differential rotation is distributed throughout the convection zone. The most significant differences in rotation occur between different latitudes; in addition, a small radial rotation gradient occurs at the base of the convection zone. Differential rotation acts as a generator producing an azimuthal magnetic field from poloidal components of the field. This creates a helical field structure within the Sun with spirals of opposite signs in the northern and southern hemispheres.

Figure 4 shows the net transfer of helicity into the northern and southern hemispheres, taking into account the equatorial rotation. The data shown in Figure 3 give $\dot{H}(\mathcal{V}_N \rightarrow C_N)$ for the north corona. From (22),

$$dH_{VN}/dt = -\dot{H}(\mathcal{V}_N \rightarrow C_N) - \dot{H}(\mathcal{V}_N \rightarrow \mathcal{V}_S). \quad (33)$$

Thus, to obtain inflow into the north subsurface fields, we reverse the sign of the data in Figure 3 and subtract the equatorial transfer from north to south. Figure 4 shows a net negative inflow into the northern hemisphere and positive into the southern hemisphere. Again, the sign does not depend on which 11 year sunspot cycle the data come from. Also, as one might expect, there is maximum helicity transfer at solar minimum, when

the flux is distributed at high latitudes (and hence rotates most slowly compared to the equatorial boundary).

Recall that estimates suggest that the Sun sheds helicity at the rate of $10^{41} \text{ Mx}^2/d$, or 10^{45} Mx^2 per 11 year cycle. In comparison, the net inflow to each hemisphere is an order of magnitude larger: the northern hemisphere receives, on average, $-5 \times 10^{42} \text{ Mx}^2/d$, or $-2 \times 10^{46} \text{ Mx}^2$ for an 11 year cycle. The south gets even more: $6.5 \times 10^{42} \text{ Mx}^2/d$, or $2.5 \times 10^{46} \text{ Mx}^2$ for an 11 year cycle. These are rates of change of the magnetic helicity stored deep in the convection zone. However, one might infer from these values that the actual helicity stored is quite high. Possibly only a small fraction escapes to the surface with rising flux tubes, to endow coronal structures with their characteristic hemisphere-dependent patterns.

As mentioned in section 2, the helicity input to a hemisphere can be decomposed into different azimuthal m modes, but the poloidal ℓ modes cannot be separated. Figure 5 shows the $m = 1, 2$ modes for helicity flow into the north solar interior. These modes provide only a few percent of the total helicity flow; the axisymmetric part of the flux distribution acted on by differential rotation provides by far the dominant contribution. We note that the solar magnetogram data do not distinguish between open and closed coronal fields. Thus some of the negative helicity flow into the north interior of the Sun results from positive helicity flow into active regions sheared by the differential rotation. Presumably, the higher m modes pick up more of the active region flux, while low m modes are most sensitive to structures on the largest scales, such as coronal holes. The graphs show that the nonaxisymmetric modes seem to be strongest at solar maximum, in contrast to the total helicity flow, which is strongest at solar minimum.

6. Conclusions

The recent observational evidence for negative magnetic helicity in the northern corona and positive helicity in the southern corona points to a need for understanding in detail the distribution of helicity in the Sun and its environment. Recent theoretical models [*van Ballegooijen & Martens* 1990, *Priest et al.* 1996, *van Ballegooijen et al.* 1998] have studied the action of differential rotation as it shears the foot points of coronal structures. These models do not give a clear hemispheric dependence, suggesting that coronal flux emerges already carrying the proper sign of helicity [*Low* 1994]. Thus we must look at dynamo theory for guidance.

Classical dynamo models of the Sun involve both the α effect from kinetic helicity and the Ω effect from differential rotation. Both of these effects can have profound influences on the magnetic helicity distribution. The α effect contribution presents great theoretical difficulties. In contrast, as we have shown, helicity generation by the Ω effect can be expressed as a simple surface integral and can thus be measured directly from solar observations. The Ω effect generates toroidal flux from the poloidal field; the α effect performs the complementary task of regenerating poloidal flux from the toroidal field. One might guess that both effects generate significant amounts of magnetic

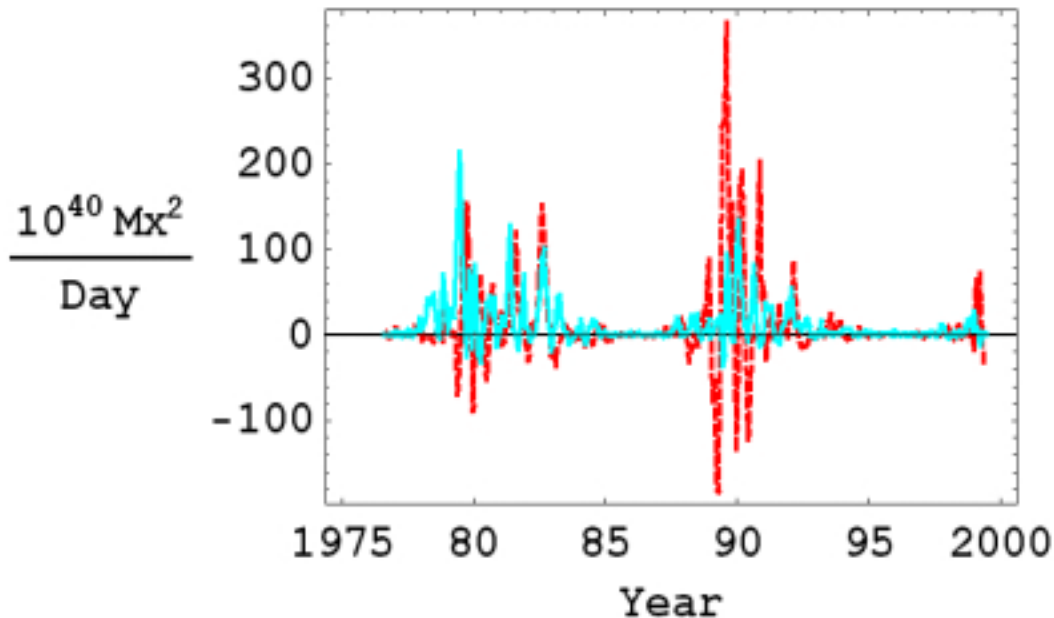


Figure 5. Helicity transfer into the northern interior for nonaxisymmetric modes. The $m = 1$ contribution is given by a dotted line, while $m = 2$ is a solid line. The units are $10^{40} \text{ Mx}^2/\text{day}$.

helicity. However, this paper concentrates on the Ω contribution simply because it can be obtained directly from observations.

The Ω effect involves the twisting up of the interior magnetic field by differential rotation [Babcock 1961, Rust 1997]. This effect produces helicity of the correct sign in each hemisphere (see figure 4), independent of cycle. The net inflow to a hemisphere is large: on average, $-5 \times 10^{42} \text{ Mx}^2/d$, or $-2 \times 10^{46} \text{ Mx}^2$ for an 11 year cycle to the northern hemisphere ($6.5 \times 10^{42} \text{ Mx}^2/d$, or $2.5 \times 10^{46} \text{ Mx}^2$ for the south). Thus one may expect that subsurface fields store helicity of the correct sign. We need only some 10% of this magnetic helicity input to account for estimates of the helicity shed in mass ejections. The magnetic helicity stored at the base of the convection zone can be carried to the surface in rising flux tubes.

Where does the rest of the helicity go? Each solar hemisphere has only one other boundary besides the photosphere: the equator. We have suggested that turbulent diffusion caused by small-scale flows can transfer helicity between the northern and southern hemispheres. The negative helicity of the north cancels with the positive helicity of the south. Crude estimates of this process suggest it may be comparable in magnitude to the helicity generation by differential rotation. An alternative possibility is helicity dissipation. However, this requires sending negative helicity to small scales. This probably can be done only if the predominant sign of α is positive. In this case,

large-scale fields would acquire positive magnetic helicity. There are two difficulties with this scenario. First, if the α contribution to helicity generation is stronger at some parts of the solar cycle than the Ω contribution, then one would expect to see positive helicity in north coronal structures. Second, because magnetic helicity has the tendency to inverse cascade, the dissipation of magnetic helicity may be inefficient.

We have also calculated the total magnetic helicity sent into the solar wind by solar rotation. This helicity manifests itself in the shape of the Parker spiral. The calculations presented here complement those of *Bieber et al.* [1987a]; we calculate the flow of helicity as it passes through the solar surface, while the earlier paper estimated the net magnetic helicity of a section of the solar wind. The two approaches are in excellent agreement.

Acknowledgments

Wilcox Solar Observatory data used in this study were obtained via the Web site <http://quake.Stanford.EDU/~wso> courtesy of J. T. Hoeksema. The Wilcox Solar Observatory is supported by NASA, NSF, and ONR. We are happy to acknowledge discussions with W. Matthaeus, D. Rust, C. Smith, and P. Laurence. Part of this work was funded by PPARC grant GR/L63143.

Michel Blanc thanks three referees for their assistance in evaluating this paper.

M. A. Berger, Department of Mathematics, University College London, Gower Street, London WC1E 6BT, United Kingdom (m.berger@ucl.ac.uk)

A. Ruzmaikin, Jet Propulsion Laboratory, California Institute of Technology, 4800 Oak Grove Dr., Pasadena, CA 91109, USA. (aruzmaik@jpl.nasa.gov)

References

- [Arnold & Khesin 1998] Arnold, V. I. & B. A. Khesin, *Topological Methods in Hydrodynamics*, New York: Springer, 1998.
- [Babcock 1961] Babcock, H. W. 1961 The topology of the sun's magnetic field and the 22 year cycle *Astrophys. J.* 133 572
- [Berger 1984] Berger, M. A. 1984 Rigorous new limits on magnetic helicity dissipation in the solar corona *Geophys. Astrophys. Fluid Dyn.* 30 79
- [Berger 1991] Berger, M. A. 1991 Generation of magnetic field structure by random boundary motions. I. mean square twist and current density *Astron. Astrophys.* 252 369
- [Berger & Field 1984] Berger, M. A. & G. B. Field 1984 The topological properties of magnetic helicity *J. Fluid Mech.* 147 133
- [Bieber et al. 1987a] Bieber, J. W., P. A. Evenson, & W. H. Matthaeus 1987 Magnetic helicity of the Parker field *Astrophys. J.* 315 700
- [Bieber et al. 1987b] Bieber, J. W., P. A. Evenson, & W. H. Matthaeus 1987 Magnetic helicity of the IMF and the solar modulation of cosmic rays *Geophys. Res. Lett.* 14 864
- [Bogomolov 1979] Bogomolov, V. A. 1979 Two-dimensional fluid dynamics on a sphere *Izv. Acad. Sci. USSR Atmos. Oceanic Phys., Engl. Transl.* 15 18

- [Brandenburg et al. 1990] Brandenburg, A., I. Tuominen, A. Nordlund, P. Pulkinen, & R. F. Stein 1990 3-D simulation of turbulent cyclonic magneto-convection *Astron. Astrophys.* 232 277
- [Brown et al. 1999] Brown, M. R., R. C. Canfield, & A. A. Pevtsov (Eds.), *Magnetic Helicity in Space and Laboratory Plasmas, Geophys. Monogr. Ser.*, vol. 111, AGU, Washington, D.C., 1999.
- [Brummell et al. 1997] Brummell, N. H., N. E. Hurlburt & J. Toomre 1997 Turbulent compressible convection with rotation. II. mean flows and differential rotation *Astrophys. J.* 493 955
- [Ding et al. 1987] Ding, Y. J., Q. F. Hong, & H. Z. Wang 1987 A statistical study of the spiral spots on the solar disc *Sol. Phys.* 107 221
- [Finn & Antonsen 1985] Finn, J., & T. M. Antonsen 1985 Magnetic helicity: what is it, and what is it good for? *Comments Plasma Phys. Controlled Fusion.* 9 111
- [Hoeksema et al. 1983] Hoeksema, J. T., J. M. Wilcox, & P. H. Scherrer 1983 The structure of the heliospheric current sheet: 1978-1982 *J. Geophys. Res.* 88 9910
- [Karpen et al. 1993] Karpen, J. T., S. K. Antiochos, R. B. Dahlburg, & D. S. Spicer 1993 The Kelvin-Helmholtz instability in photospheric flows - effects of coronal heating and structure *Astrophys. J.* 403 769
- [Kimura & Okamoto 1987] Kimura, Y. & H. Okamoto 1987 Vortex motion on a sphere *J. Phys. Soc. Jpn.* 56 2024
- [Kosovichev et al. 1997] Kosovichev, A. G., et al. 1997 Structure and rotation of the solar interior: initial results from the MDI Medium-L program *Sol. Phys.* 170 43
- [Kumar & Rust 1996] Kumar, A. & D. M. Rust Interplanetary magnetic clouds, helicity conservation, and current-core flux ropes 1996 *J. Geophys. Res.* 101 15,667
- [Krause & Rädler 1981] Krause, F., & K.-H. Rädler, *Mean-Field Dynamo and Mean-Field Magnetohydrodynamics*, Springer-Verlag, New York, 1981.
- [Low 1994] Low, B. C. 1994 Magnetohydrodynamic processes in the solar corona - flares, coronal mass ejections, and magnetic helicity *Physics Plasmas* 1 1684
- [Low & Hundhausen 1995] Low, B. C. & J. R. Hundhausen 1995 Magnetostatic structures of the solar corona. 2: The magnetic topology of quiescent prominences *Astrophys. J.* 443 818
- [Martin et al. 1992] Martin, S. F., et al. 1992 The solar cycle pattern in the direction of the magnetic field along the long axes of polar filaments, in *The Solar Cycle* ASP Conf. Ser., vol. 27, edited by K. L. Harvey, pp. 53, Astron. Soc. of the Pac., San Francisco, Calif.
- [Martin & McAllister 1997] Martin, S. F., & A. H. McAllister 1997 predicting the sign of magnetic helicity in erupting filaments and coronal mass ejections, in *Coronal Mass Ejections* Geophys. Monogr. Ser., vol. 99, edited by Crooker, N., J. A. Joselyn and J. Feynman, pp. 127-138, AGU, Washington D.C.
- [Matthaeus & Montgomery 1980] W. H. Matthaeus & D. Montgomery 1980 Selective decay hypotheses at high mechanical and magnetic Reynolds numbers *Ann. N. Y. Acad. Sci.* 357 203
- [Moffatt 1978] H. K. Moffatt, *Magnetic Field Generation in Electrically Conducting Fluids*, Cambridge Univ. Press, New York, 1978.
- [Moffatt & Ricca 1992] H. K. Moffatt & R. L. Ricca 1992 Helicity and the Calugareanŭ invariant *Proc. R. Soc. London, Ser. A* 439 411
- [Parker 1983] Parker, E. N. 1983 Magnetic neutral sheets in evolving fields. II - Formation of the solar corona *Astrophys. J.* 264 642
- [Parker 1993] Parker, E. N. 1993 A solar dynamo surface wave at the interface between convection and nonuniform rotation *Astrophys. J.* 408 707
- [Pevtsov et al. 1995] Pevtsov, A. A., R. C. Canfield, & T. R. Metcalf 1995 Latitudinal variation of helicity of photospheric fields *Astrophys. J.* 440 L109
- [Pouquet et al. 1976] Pouquet, A., U. Frisch, & J. Léorat 1976 Strong MHD helical turbulence and the nonlinear dynamo effect *J. Fluid Mech.* 77 321
- [Priest et al. 1996] Priest, E. R., A. A. van Ballegoijen, & D. H. Mackay 1996 Model for dextral and sinistral prominences *Astrophys. J.* 460 530
- [Richardson 1941] Richardson, R. S. 1941 The nature of solar hydrogen vortices *Astrophys. J.* 93 24

- [Rust 1994] Rust, D. M. 1994 Spawning and shedding helical magnetic fields in the solar atmosphere *Geophysical Research Letters* 21 241
- [Rust 1997] Rust, D. 1997 Helicity Conservation, in *Coronal Mass Ejections* Geophys. Monogr. Ser., vol. 99, edited by Crooker, N., J. A. Joselyn and J. Feynman, pp. 119-125, AGU, Washington D.C.
- [Rust & Kumar 1994] Rust, D. M. & A. Kumar 1994 Helical magnetic fields in filaments *Sol. Phys.* 155 69
- [Rust 1994] Rust, D. M. & Martin, S. F. 1994 A Correlation Between Sunspot Whirls and Filament Type, in *Solar Active Region Evolution* ASP Conf. Ser., vol. 68, edited by K. S. Balasubramaniam & G. W. Simon, pp. 337-338, Astron. Soc. of the Pac., San Francisco, Calif.
- [Ruzmaikin 1996] Ruzmaikin, A. 1996 Redistribution of magnetic helicity at the Sun *Geophys. Res. Lett.* 23 2649
- [Seehafer 1990] Seehafer, N. 1990 Electric current helicity in the solar atmosphere *Sol. Phys.* 125 219
- [Seehafer 1996] Seehafer, N. 1996 Nature of the α effect in magnetohydro-dynamics *Phys. Rev. E* 53 1283
- [Sturrock & Uchida 1981] Sturrock, P. A. & Y. Uchida 1981 Coronal heating by stochastic magnetic pumping *Astrophys. J.* 246 331
- [van Ballegooijen & Martens 1990] van Ballegooijen, A. A., & P. C. H. Martens 1990 Magnetic fields in quiescent prominences *Astrophys. J.* 361 283
- [van Ballegooijen et al. 1998] van Ballegooijen, A. A., N. P. Cartledge, & E. R. Priest 1998 Magnetic flux transport and the formation of filament channels on the sun *Astrophys. J.* 501 866
- [Wang 1993] Wang, Y. M. 1993 On the latitude and solar cycle dependence of the interplanetary magnetic field strength *J. Geophys. Res.* 98 3529
- [Zeldovich et al. 1983] Zeldovich, Y. B., A. A. Ruzmaikin, and D. D. Sokoloff, *Magnetic Fields in Astrophysics*, Gordon and Breach, Newark, N. J., 1983.
- [Zhao & Hoeksema 1993] Zhao, X. P., & J. T. Hoeksema 1993 Unique determination of model coronal magnetic fields using photospheric observations *Sol. Phys.* 143 41
- [Zhao & Hoeksema 1995] Zhao, X. P., & J. T. Hoeksema 1995 Prediction of the interplanetary magnetic field strength *J. Geophys. Res.* 100 19